ELSEVIER

Surface Science 387 (1997) 328–341

surface science

Activation of O_2 on Cu, Ag, and Au surfaces for the epoxidation of ethylene: dipped adcluster model study

Hiroshi Nakatsuji [a,b,c,*], Zhen-Ming Hu [a], Hiromi Nakai [a,1], Keiji Ikeda [a]

[a] *Department of Synthetic Chemistry and Biological Chemistry, Graduate School of Engineering, Kyoto University, Sakyo-ku, Kyoto, 606-01, Japan*

[b] *Department of Applied Chemistry, Graduate School of Engineering, The University of Tokyo, Hongo, Tokyo, 113, Japan*

[c] *Institute for Fundamental Chemistry, 34-4, Takano-Nishihirakicho, Sakyo-ku, Kyoto, 606, Japan*

Received 17 September 1996; accepted for publication 28 April 1997

Abstract

Aiming to clarify why only silver is an effective catalyst for the partial oxidation of ethylene, we studied theoretically the reactivity and the stability of oxygen species on Cu, Ag, and Au surfaces. We used the dipped adcluster model (DAM), since electron transfer from metal to oxygen is important, and the SAC/SAC-CI method, since several electronic states are involved. We found that if superoxide species exists on the surface, both Cu and Au surfaces show a reactivity similar to Ag surface, leading smoothly to ethylene oxide, and the barriers leading to complete oxidations should be very high. Therefore, the point is the relative stability of the various oxygen species and, in particular, the stability of the superoxide species on the metal surface. On Cu, superoxide is much less stable than peroxide, which again is less stable than the dissociated species, and no barrier exists for the conversion from superoxide to peroxide. On Au, our DAM calculations show that the electron flow from the bulk metal into the adcluster does not occur, so that the molecularly adsorbed oxygen species, as well as the dissociative ones, find it difficult to exist stably on the clean surface. On Ag, superoxide should certainly have some life time to react with ethylene to give ethylene oxide, which is considered to be the origin of the unique catalytic activity of silver for the epoxidation of ethylene. This is related to the ability of electron transfer and to the geometry of the Ag surface. We have proposed a basic idea for a new catalytic design of the epoxidation reaction.

Keywords: Copper; Dipped adcluster model (DAM); Epoxidation of ethylene; Gold; Oxygen chemisorption; Peroxide; Reactivity; SAC/SAC-CI method; Silver; Stability; Superoxide

1. Introduction

The stabilities and reactivities of oxygen species adsorbed on the Group 1B-metal (Cu, Ag, Au) surfaces have received much attention because of their importance in catalysis study and surface science [1,2]. Oxygen species on an Ag surface causes the catalytic oxidation of ethylene to ethylene oxide, and those on Ag and Cu surfaces convert methanol into formaldehyde [3–6]; both are quite important and useful reactions in industrial chemistry. However, Cu and Au surfaces are not good catalysts for the former reaction, and an Au surface is not good for the latter reaction, though it was found by Haruta et al. that Au is

* Corresponding author.

[1] Present address: Department of Chemistry, School of Science and Engineering, Waseda University, Ohkubo 3-4-1, Shinjuku-ku, Tokyo, 169, Japan.

0039-6028/97/$17.00
PII S0039-6028(97)00368-3

remarkably active for the oxidation of CO [7] and the selective oxidation of hydrocarbons [8] when it is supported on suitable metal oxides.

In a previous study, we showed theoretically that the end-on superoxide on an Ag surface is highly selective and active for the partial oxidation of ethylene [9]. The dissociated oxygen species is not so selective; it gives both ethylene oxide and acetaldehyde [9], the latter being further oxidized to CO_2 and H_2O. It is important to clarify and compare the activation mechanisms of O_2 on Cu, Ag, and Au surfaces to understand the differences in the catalytic activities on these metal surfaces.

Experimental researches of O_2 on an Ag surface have revealed the existence of at least five adsorbed species: physisorbed, two molecularly chemisorbed (superoxide and peroxide), dissociatively chemisorbed and subsurface states [10–18]. In contrast, the nature of O_2 on a Cu surface has not yet been clearly identified: there is some dispute over the existence of a molecularly chemisorbed species. Early work by Spitzer and Luth showed the existence of molecular species on a single crystal Cu surface [19]. Prabhakaran and coworkers [20] found a molecular species with an O–O stretching frequency of 660 cm^{-1} on the Cu(110) surface at 80 K, and two molecular species with O–O stretching frequencies of 610 and 880 cm^{-1} on the polycrystalline Cu surface. However, Mundenar et al. found no evidence of molecular adsorption on the Cu(110) surface [21]. On the other hand, the dissociative chemisorption of O_2 on the Cu(110) surface has been generally accepted [1,22]. A $[2 \times 1]$ low energy electron diffraction (LEED) pattern with the oxygen atom occupying a long bridge site has been reported on the Cu(110) surface, as on the Ag(110) surface. Gold has been thought to be one of the least active metals for chemisorption; oxygen seems not to be chemisorbed either molecularly and dissociatively on a clean Au surface [23–26]. However, when it is supported on suitable metal oxides, gold seems to show much reactivity [7,8].

Several theoretical papers have been published studying the interactions of O_2 with an Ag surface [27–35], but only a few have studied the Cu surface [36–38]. Our previous studies have shown the importance of electron transfer, electrostatic interaction, and electron correlations for O_2 chemisorption on an Ag surface [34,35]. In the conventional cluster model, very large clusters must be used to describe O_2 chemisorption on a metal surface, but the dipped adcluster model (DAM) [39,40] can describe the effects of bulk metal quite naturally in a simple theoretical framework. Further, for studying different electronic states on a surface, like a peroxide and a superoxide, we need a theory which can describe both ground and excited states to a similar accuracy. The symmetry-adapted cluster (SAC)/SAC-configuration interaction (SAC-CI) method [41–44] is such a theory. We have succeeded in describing both molecular (side-on) and dissociative adsorptions of oxygen on the Ag surface [34,35] by using the DAM combined with the SAC/SAC-CI method.

In this study, we compare Cu, Ag, and Au surfaces for the chemisorption and activation of O_2 molecule. We study molecular end-on and side-on adsorptions, dissociative adsorptions, their electronic structures, and frontier-orbital properties. The reactions of the superoxide species with ethylene to form ethylene oxide are studied for Cu and Au surfaces and compared with the previous result on an Ag surface [9]. We want to clarify the reason why only silver is a good catalyst for the partial oxidation of ethylene.

2. Computational details

DAM [39,40] is a model for studying chemisorptions and surface reactions involving electron transfer between an admolecule and a surface, and the image force is considered for the reaction on a metal surface. This model has been applied successfully to the adsorptions of O_2 on Pd and Ag surfaces [34,35,39,40] for which the conventional cluster model failed. Then, we adopt the DAM for the present study and investigate molecular adsorption of O_2 on Cu, Ag, and Au surfaces assuming one-electron transfer from the bulk metal into the adcluster. Thereafter, we reinvestigate this electron transferability for these surfaces by examining the condition given by the DAM, and an

exceptional nature of the Au surface will be clarified.

We take M_2O_2 and M_4O_2 (M = Cu, Ag, Au) as adclusters, in which the M–M distances are fixed at their lattice constants: 2.556 Å, 2.8894 Å, and 2.8841 Å for Cu, Ag, and Au respectively [45]. Both molecular end-on and side-on adsorptions are studied using the M_2O_2 adcluster, and conversions between the molecular and dissociative adsorptions are examined using the M_4O_2 adcluster.

The geometries of the molecular end-on and side-on species, as well as those appearing in the partial oxidation reaction pathways of ethylene to ethylene oxide, are optimized at the unrestricted Hartree–Fock (UHF) level. The electron correlations are further considered by using the MP2 method to calculate the energy diagrams of the partial oxidation reactions. The SAC/SAC-CI method is used to calculate the energy curves in the conversion processes between end-on and side-on forms shown in Section 3.2, as well as in oxygen elongation and dissociation processes shown in Sections 3.3 and 5 respectively, since the roles of lower ground and excited states are quite important in these kinds of surface electronic process [34,35].

The active spaces in the SAC/SAC-CI calculations are composed of 72 MOs (16 occ + 56 unocc) and 112 MOs (27 occ + 85 unocc) for the M_2O_2 and M_4O_2 adclusters respectively. The active occupied orbitals are composed of the d and s orbitals of the metals and the 2p orbitals of O. The 1s and 2s orbitals of O, as well as their counterparts in the unoccupied space, are frozen. In the SAC calculations, double-excitation operators whose second-order perturbation energies with the HF configuration are larger than 3×10^{-5} Hartree are included [46]. In the SAC-CI calculations, a threshold of 1×10^{-5} Hartree is used for the ionized state calculations [46]. The HF calculations are carried out using the HONDO program [47], and the SAC/SAC-CI calculations using the SAC85 program [48].

The Gaussian basis sets for Cu, Ag, and Au are [3s2p2d] with the relativistic effective core potentials [49]. For oxygen, we use the Huzinaga–Dunning (9s5p)/[4s2p] set [50,51] augmented by the diffuse s and p functions of $\alpha =$ 0.059 [52] in all of the calculations for geometry optimization, and the polarization d functions of $\alpha = 1.154$ [53] are further augmented in the DAM and SAC/SAC-CI calculations. For comparison, the same two polarization d functions of $\alpha = 2.704$ and 0.535 [53], as used in the previous study [9], are used to calculate the energy diagrams at the MP2 level. For carbon and hydrogen, the respective sets (9s5p)/[4s2p] and (4s)/[2s] of Huzinaga–Dunning are adopted. We have already shown that these basis sets are reliable for studying the energetics along the surface reactions [9]. A comparative study of the Ag 19-electron RECP and 11-electron RECP for Ag_2 and AgO, performed by Hay and Martin [54], has shown that the inclusion of the 4s and 4p shell produced slightly longer bond lengths but left the spectroscopic constants, such as stretching frequency and dissociation energy, virtually unchanged.

3. Molecular O_2 adsorption

3.1. End-on adsorption and the reactivity of superoxide

The experimental results show that only silver is a good catalyst for the partial oxidation of ethylene to ethylene oxide. In a previous study [9], we showed that the superoxide species adsorbed in the end-on form on an Ag surface is very active and selective for the epoxidation reaction. In this section, we examine the electronic structure and the reactivity of the end-on species on the Cu and Au surfaces and compare them with those on the Ag surface.

Table 1 shows the optimized geometry for the end-on adsorption of O_2 on Cu_2, Ag_2, and Au_2 surfaces calculated by the UHF method. Fig. 1 shows an illustration of the geometry of the end-on form. One-electron transfer from the bulk to the adcluster was considered by the DAM; i.e. $n = 1$. In the optimizations, the $O_aM_aM_b$ angle was fixed at 90°. The calculated adsorption energy is all positive, showing stable end-on adsorption to occur. The results for Au may contradict the experimental ones since the Au surface may not adsorb O_2 molecule.

Table 1
Adsorption energies and UHF optimized geometries of the end-on superoxide species on Cu, Ag, and Au surfaces

System	Adsorption energy (kcal mol^{-1})		R_{M-O} (Å)	R_{O-O} (Å)[a]	ϕ_{OOM} (deg)	ϕ_{OMM} (deg)
	UHF level	MP2 level				
Cu_2O_2	13.7	31.4	2.107	1.360	114.9	90.0 (fixed)
Ag_2O_2	7.4	26.9	2.340	1.389	113.4	90.0 (fixed)
Au_2O_2	5.1	29.8	2.349	1.364	111.9	90.0 (fixed)

[a] R_{O-O} of free O_2 anion (O_2^-) is 1.65 Å.

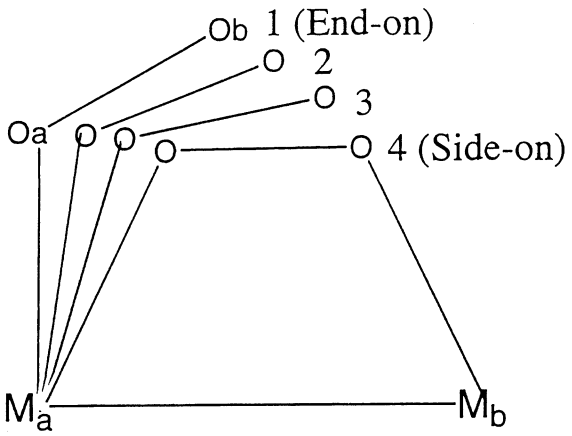

Fig. 1. Illustration of the geometrical conversion from end-on (#1) to side-on (#4) forms. The M–M (M=Cu, Ag, and Au) distances were fixed at the lattice constants.

The calculated OOM angles are close to each other. The O–O distances of 1.35 to 1.38 Å are close to or slightly greater than that of a free O_2 anion (1.35 Å) [55]. The Cu–O distance of 2.10 Å is shorter than the Au–O and Ag–O distances, reflecting a large adsorption energy and a short lattice constant of Cu.

The calculated electronic structure of O_2 in the end-on adsorption form is superoxide O_2^- with the symmetry of $^2A'$. Table 2 shows the net charge and frontier density (or spin population) which are related to the reactivity. In all three species, the net charges on the inside (O_a) and outside (O_b) oxygen atoms are calculated to be about −0.6 and −0.15 respectively, while the outside oxygen atoms have a frontier density of about 0.86, which is much larger than that of the inside oxygen atoms (about 0.12). This shows that the outside oxygen is much more reactive than the inside one and that the former is not so negative as the latter one, the same result as that reported before [35] for a linear Ag–O–O system. Actually, in the epoxidation reaction with ethylene, the oxygen which reacts with ethylene is the outside one [9]. Based on the analyses of the net charge and the frontier density, similar reactivity is expected for the end-on superoxide species on Cu, Ag, and Au surfaces.

For the selective oxidation of ethylene to ethylene oxide, only silver is a good catalyst. However, it is not yet well understood why only silver is so exceptional, nor is it understood which adsorbed oxygen species (atomic vs. molecular) is active for the reaction. In a previous report [9], we studied the mechanism of the partial oxidation of ethylene on an Ag surface and elucidated the end-on super-

Table 2
Net charge and frontier density of the end-on superoxide species on Cu, Ag, and Au surfaces

System[a]	Net charge				Frontier density			
	M_a	M_b	O_a	O_b	M_a	M_b	O_a	O_b
Cu_2O_2	+0.060	−0.271	−0.643	−0.146	0.007	0.002	0.133	0.858
Ag_2O_2	+0.058	−0.295	−0.605	−0.158	0.014	0.003	0.119	0.864
Au_2O_2	+0.095	−0.285	−0.644	−0.166	0.007	0.002	0.116	0.876

[a] The geometry of the end-on form is shown in Fig. 1.

oxide to be an active oxygen species. We examine here the reactivity of the end-on superoxide species on Cu and Au surfaces for the partial oxidation of ethylene and compare this with the result for the Ag surface [9].

Fig. 2 shows the energy diagrams and the geometries of the intermediates and the transition states for the reactions of ethylene on Cu, Ag, and Au surfaces leading to ethylene oxide and acetaldehyde. This reaction process is similar to the one studied in detail for the oxidation reaction of ethylene on a silver surface [9]. Since the optimized geometries obtained in the reaction pathways are very similar, only the characteristic geometries are listed in Fig. 2 for simplicity. The energy diagrams were calculated by the MP2 method, since the electron correlation is important in this kind of reaction. We see that the energy profiles for the reactions are similar to each other on all the metal surfaces and imply a two-step mechanism of the reactions. The first step is the adsorption of O_2 in a superoxide form and the second step is the reaction of the superoxide with ethylene. The energy barrier for the second step, which seems to be the rate-determining step, is about 11 kcal mol^{-1} at R_{CO} of about 1.78 Å: outside oxygen reacts with the carbon of ethylene. The energy barrier is similar for all the metals studied here. At the intermediate, the C–O distance is 1.43 Å, which is much shorter than that in the transition state. After reaching this intermediate, the reaction leading to ethylene oxide is quite smooth.

From the above intermediate, another reaction route leading to complete oxidation exists. The calculated energy barrier for the formation of acetaldehyde, an intermediate in the complete oxidation process, is very high, about 70 kcal mol^{-1}, for all the surfaces. This implies that the complete oxidation of ethylene does not occur from the superoxide species on all the metal surfaces studied here.

The energy profiles given in Fig. 2 show that the superoxide species on Cu, Ag and Au surfaces have a quite similar reactivity for the partial oxidation of ethylene: the differences among the energy diagrams shown in Fig. 2 are too small to explain why only silver is an effective catalyst. Indeed, the present results suggest the possibility that copper and gold may also work as good catalysts for the partial oxidation of ethylene, if the end-on superoxide can exist as a stable or long-lived species on Cu and Au surfaces. However, experimentally, no observation of the superoxide species has been reported on the Cu and Au surfaces. This fact may offer a key to the understanding of the reason for the unique catalytic activity of silver.

3.2. Conversion from end-on superoxide to side-on peroxide

Next, we examine a conversion from the end-on to the side-on geometries. This process accompanies a conversion from the superoxide to the peroxide, since the ground state of the end-on and side-on species are the superoxide and peroxide respectively, as shown in some detail in this section. Thus, the method to be used here should be able to describe both ground and excited states to a good accuracy. For this purpose, the HF method is inadequate and, therefore, we use the SAC/SAC-CI method [43,44]. The geometries optimized at the HF level shown in Tables 1 and 3 are used for the end-on (#1) and side-on (#4) forms respectively. The intermediate geometries #2 and #3, which are illustrated in Fig. 1, are approximated as a linear function of the OMM angle.

Fig. 3 shows the potential energy curves (PECs) calculated for the conversion process between the end-on and side-on forms on the Cu, Ag, and Au surfaces. In the end-on geometry the superoxide ($^2B_2$) is always the ground state, but in the side-on geometry the ground state is the peroxide species ($^2A_1$). The superoxide species with the $^2A_2$ symmetry is less important, since it never becomes the ground state in this conversion process. In the $^2B_2$ superoxide, the in-plane π^* orbital of oxygen is singly occupied and the out-of-plane π^* orbital is doubly occupied. These occupations are reversed in the $^2A_2$ state. The crossing of the PECs of the superoxide and peroxide occurs between the end-on and side-on geometries.

The relative stabilities of the superoxide and peroxide in the end-on and side-on geometries and the barrier of the conversion are quite important for understanding the catalytic activities of metals

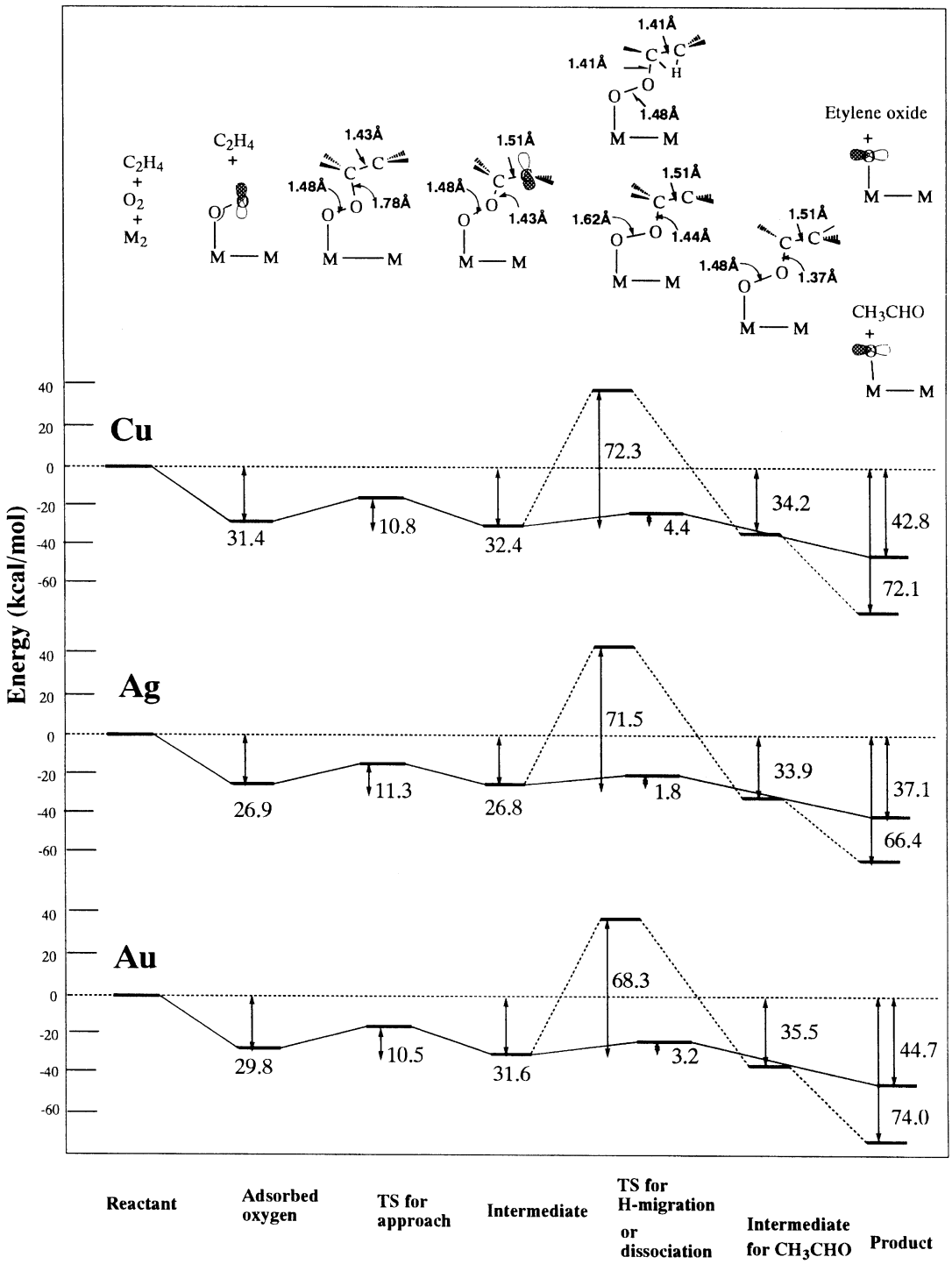

Fig. 2. Energy diagram for the formation of ethylene oxide (——) and of acetaldhyde (- - -) from ethylene by the end-on superoxide species on Cu, Ag, and Au surfaces calculated by the MP2 method.

Table 3
Gross charge and optimized geometry of the side-on peroxide on Cu, Ag, and Au surfaces by the UHF method

System	Net charge on O	$R_{M\text{-}O}$ (Å)	$R_{O\text{-}O}$ (Å)	ϕ_{OOM} (deg)	ϕ_{OMM} (deg)
Cu_2O_2	−0.632	1.9393	1.5164	105.55	74.45
Ag_2O_2	−0.631	2.1420	1.5090	108.79	71.21
Au_2O_2	−0.454	2.1563	1.5082	108.6	71.4

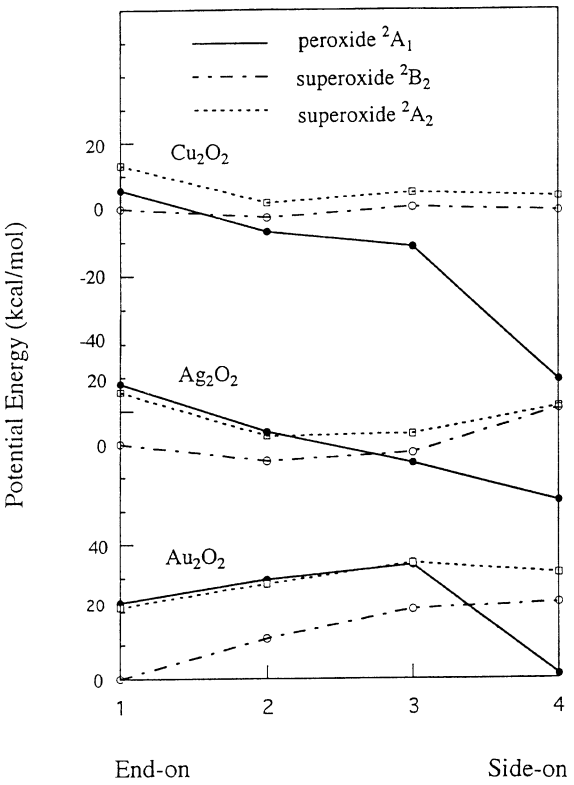

Fig. 3. PECs calculated by the SAC/SAC-CI method for the conversion between the end-on (#1) and side-on (#4) adsorption states in the lowest three states of the Cu_2O_2, Ag_2O_2, and Au_2O_2 adclusters with $n=1$.

for the partial oxidation of ethylene. Such information is given in Fig. 3. In the end-on form, the superoxide species is more stable than the peroxide species: the energy difference is about 20 kcal mol^{-1} for Ag and Au and 5 kcal mol^{-1} for Cu. In the side-on form, the peroxide species is more stable than the superoxide species: the energy difference is 50.1 kcal mol^{-1}, 27.6 kcal mol^{-1}, and 21.2 kcal mol^{-1} for Cu, Ag, and Au respectively. The energy difference between the end-on superoxide and the side-on peroxide is 50.8 kcal mol^{-1}, 23.1 kcal mol^{-1}, and −1.2 kcal mol^{-1} for Cu, Ag, and Au respectively. On the Cu surface, the superoxide species in the end-on form converts easily into the peroxide species in the side-on form because of a large stabilization energy and the lack of a barrier: the lifetime of the end-on superoxide species should be very short on the Cu surface. On the other hand, an energy barrier of about 20 kcal mol^{-1} is calculated for the conversion on Au, and a considerable lifetime is expected for the end-on superoxide on Ag, as seen from the PECs shown in Fig. 3.

In the adsorption of O_2 on these surfaces, the O_2 molecule would initially be adsorbed in an end-on form from both energetics and dynamics: the probability of approaching in the end-on form should be larger than that in the side-on form. On the Ag and Au surfaces, this superoxide species would have a lifetime during which it is attacked by the reagent, like ethylene, but on Cu the lifetime would be too short to receive an attack by the reagent. This may explain the selectivity of Ag and the non-selectivity of Cu for the partial oxidation of ethylene. On Cu, the non-selectivity is actually due to the atomic oxygen dissociatively adsorbed on the surface, as will be seen in Section 3.3. However, for Au, the results obtained from Figs. 2 and 3 do not give a clear explanation for its inability to undergo this reaction. As far as one-electron transfer from the bulk metal into the adcluster occurs for Cu, Ag, and Au, the reactivity of the superoxide on these metals should be similar. We will examine in Section 4 the electron transferability difference of these metals.

The difference in the relative stability of the superoxide O_2^- and peroxide O_2^{2-} species on a different metal is understood to be parallel with the electron-donating ability of the metal surfaces.

Fig. 4 shows the MO energy level diagram. The energy level of the HOMO is lower in Au_2 than in Cu_2 and Ag_2, and the same trend is also seen in the M_4 clusters. The work functions of the Au(110) and Au(111) surfaces are 5.37 eV and 5.31 eV respectively, which are larger than those of the Ag and Cu surfaces: i.e. Ag(110) 4.52 eV; Ag(111) 4.74 eV; Cu(110) 4.48 eV; Cu(111) 4.94 eV [45]. As a result, as shown in Table 3, the net charge of the oxygen atom in the side-on peroxide is −0.454 on the Au surface, compared with −0.632 and −0.631 on the Cu and Ag surfaces respectively. The electron donating abilities of the copper and silver surfaces seem to be similar; however, the peroxide species on the copper surface is more stable than that on the silver surface. A possible explanation is based on the difference in the ionic bond radii between copper (0.72 Å) and silver (0.89 Å). The shorter bond radii of copper results in larger chemical and image-force interactions. Indeed, the image force of the peroxide species in the side-on form on a Cu surface is calculated to be larger by 5.6 kcal mol^{-1} than that on an Ag surface.

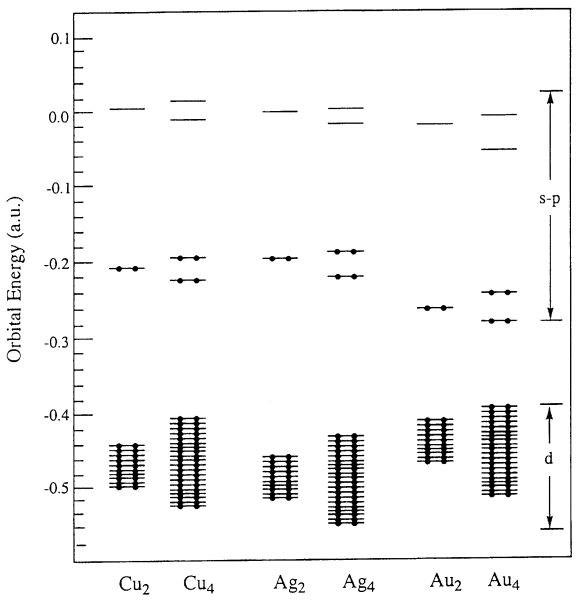

Fig. 4. The valence orbital energies of the d and s levels of free M_2 and M_4 clusters (M=Cu, Ag, and Au) calculated by the HF method.

3.3. Side-on adsorption

Here we examine another stable geometry of molecular adsorption of O_2; i.e. side-on adsorption. Table 3 shows the optimized geometries of the side-on species on the Cu, Ag, and Au surfaces calculated by the UHF method keeping the C_{2v} symmetry. The calculated Cu–O distance of 1.94 Å is about 0.2 Å shorter than the Ag–O and Au–O distances, as in the end-on geometry. The O–O distances are close to each other, but longer than those for the end-on species, reflecting the fact that the ground-state electronic structure of the side-on species is peroxide, O_2^{2-}, while that in the end-on form is superoxide, O_2^-. Note that the superoxide species are the excited states in the side-on form, as shown previously for the O_2/Ag system by the SAC-CI method [34].

For the peroxide species, there is no spin on the oxygen atoms and the charge polarization does not occur for symmetry reasons. The O–O stretching frequencies of the peroxide species were observed on Cu and Ag surfaces [11,12]. In the present study, we calculated the PECs of O_2 on Cu and Au surfaces, see Fig. 5. The M–M distances were fixed at the lattice distances, the M–O distances were fixed at the optimized distances, and the O–O distance was elongated from 1.20 to 2.55 Å on Cu and from 1.20 to 2.88 Å on Au, keeping the C_{2v} symmetry.

Fig. 5 shows that on all metal surfaces, the peroxide O_2^{2-} species with $^2A_1$ symmetry is the ground state, and the superoxide species O_2^- with $^2A_2$ and $^2B_2$ symmetries are the lower excited states. The O–O vibrational frequencies calculated from these PECs are shown in Table 4. Those of the peroxide ($^2A_1$), and two superoxides ($^2B_2$ and $^2A_2$) are 868, 965, and 1249 cm^{-1} on the Cu surface, and 718, 952, and 1056 cm^{-1} on Au, compared with those of 689, 974, and 1055 cm^{-1} on Ag reported previously [34]. The calculated value of 868 cm^{-1} for the peroxide O_2^{2-} on Cu is similar to that on other transition metal surfaces, Pt(111) and Pd(111), and is somewhat larger than those on the noble metal surfaces, like Ag [37]. On the other hand, the experimental values are 660 cm^{-1} on the Cu(110) surface and 610 and 880 cm^{-1} on the polycrystalline Cu surface, all of

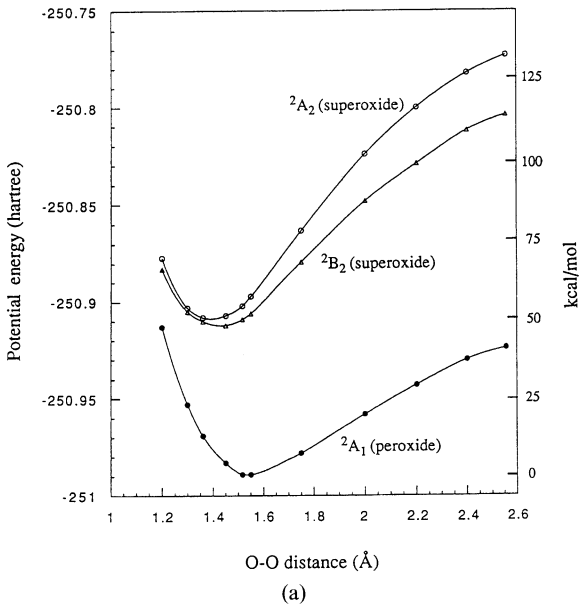

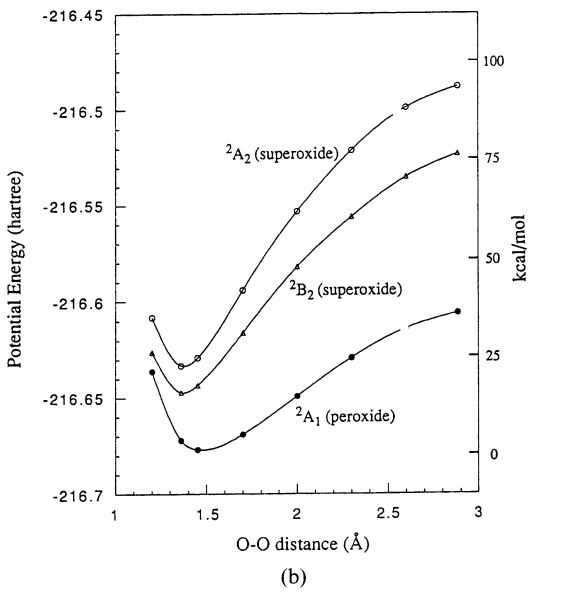

Fig. 5. PECs calculated by the SAC/SAC-CI method for the O–O elongation process in the lowest three states of (a) Cu_2O_2 and (b) Au_2O_2 adclusters with $n=1$.

which are considered to reflect the peroxide species [20]. The present calculated result of 868 cm^{-1} is close to one of the experimental results, i.e. 880 cm^{-1}. Prabhakaran and coworkers [20] pointed out that since a polycrystalline surface would contain a high proportion of (111) surface,

Table 4
The vibrational frequencies of the superoxide O_2^- and peroxide O_2^{2-} species in the gas phase and on Cu, Ag, and Au surfaces calculated by the SAC/SAC-CI method

Species	State	ω_e (cm^{-1})	Net charge of O_2
O_2^-/gas	$^2\Pi$	1066	−1
	Exptl.	1090	
O_2^{2-}/gas	$^1\Sigma_g^+$	636	−2
O_2^-/Cu	$^2A_2$	1249	−0.45
	$^2B_2$	965	−0.62
O_2^{2-}/Cu	$^2A_1$	868	−1.27
	Exptl.[a]	660, 610, 880	
O_2^-/Ag[b]	$^2A_2$	1055	−0.54
	$^2B_2$	974	−0.65
	Exptl.[c]	1053	
O_2^{2-}/Ag[b]	$^2A_1$	689	−1.40
	Exptl.[c]	628, 640, 697	
O_2^-/Au	$^2A_2$	1056	−0.19
	$^2B_2$	952	−0.53
	Exptl.[d]	1050–1150	
O_2^{2-}/Au	$^2A_1$	718	−0.91
	Exptl.[d]	740–800	

[a] Ref. [20].
[b] Ref. [34].
[c] Refs. [10–12].
[d] Ref. [25].

the value 880 cm^{-1} might be due to the (111) surface. The present M_2O_2 adcluster model may be close to the (111) surface, since on the (110) surface there is a ditch onto which O_2 can be incorporated and stabilized more by interacting with a larger number of metal atoms. Similar O–O vibrational frequencies were also obtained by using the Cu_4O_2 adcluster, as shown in Section 4.

No reliable experimental vibrational frequencies are available for the Au surface to compare with the present calculated results, although the calculated values compare well with the reported vibrational peaks, 740–800 and 1050–1150 cm^{-1}, of the HREELS spectra [25]. Pireaux et al. [25] did not interpret the data as being due to the oxygen on

an Au surface, since the possibility of contaminants could not be ruled out. However, our results on an Au surface are close to those on an Ag surface [34], indicating that the spectroscopic properties of molecular oxygen chemisorbed on an Au surface should be similar to those on an Ag surface, if electron-transfer occurs on the Au surface and the adsorbed oxygen species exist as stable species.

4. Electron transferability of gold

The results listed in Section 3 show that the oxygen superoxide species adsorbed on an Au surface has essentially the same reactivity as on Cu and Ag surfaces. The stabilities of the molecularly adsorbed oxygen species are mainly due to the electron-transfer effect from the bulk metal, as already shown previously for silver [34,35] and palladium [39,40]. The chemical potentials (work functions) of the Cu, Ag, and Au surfaces are 4.48, 4.52, and 5.37 eV for the (110) surfaces, 4.94, 4.74 and 5.31 eV for the (111) surfaces, and 4.59, 4.64, and 5.47 eV for the (100) surfaces [45]. The Cu surface is expected to have similar properties to the Ag surface, but a larger electron transferability. However, it is not clear whether the electron-transfer also occurs for the Au surface, since the electron-donating ability of the Au surface should be smaller than the others due to the larger chemical potential and the more stable s-band, as shown in Fig. 4. We therefore investigate here the $E(n)$ curves of the M_2–O_2 systems in the DAM in order to clarify why Au cannot be a good catalyst for the epoxidation of ethylene.

We take M_2O_2 (M = Cu, Ag, and Au) as adclusters. The optimized end-on geometries as listed in Table 1 are adopted, since they are the most stable geometries of the superoxide adsorbed species. At infinite separation, the O_2 molecule is in the $^3\Sigma_g^-$ state and the M_2 cluster is in the $^1\Sigma_g^+$ state. In the M_2O_2 system, the frontier MOs are composed mainly of the π^* MOs of O_2. When n electrons are transferred from the bulk metal to the adcluster, the out-of-plane π^* MO is occupied by the additional $n\beta$-spin electrons because one α-spin electron already occupies this orbital. Namely, when $n=0$ the M_2O_2 is a triplet and when $n=1$ it is a doublet.

Fig. 6 is a display of the $E(n)$ curves, namely the energy of the adcluster calculated as a function of n. It was calculated with the use of the highest spin coupling model [39]. The curves are upper convex, and at $n=1.0$ the systems are more stable than at $n=0.0$: the order of stability is $Cu_2O_2 > Ag_2O_2 > Au_2O_2$. According to the DAM [39], the electron transfer would occur between the adcluster and the bulk metal when the chemical potential of the adcluster becomes equal to the chemical potential of the solid surface, i.e. $\partial E(n)/\partial n = -\mu$. For Cu_2O_2 and Ag_2O_2 systems, the tangents of the $E(n)$ curves become equal with the experimental chemical potentials at about $n=0.9$. Therefore, from the concept of the DAM [39], one electron should flow from the Cu and Ag bulk metals into the adcluster after some barrier. However, for the Au_2O_2 system, though the energy at $n=1.0$ is lower than that at $n=0.0$, the tangent of the $E(n)$ curve is still smaller than the experimental chemical potential. Therefore, in contrast to Cu and Ag metals, one-electron flow does not occur from the Au metal into the adcluster. This point concerning the Au surface is essentially different from the other metals, and could be the reason why the molecularly adsorbed oxygen species cannot exist on a clean gold surface. As long as molecular adsorption does not occur, the dissociative adsorption following it cannot occur. Thus, the inactivity of the gold surface toward the

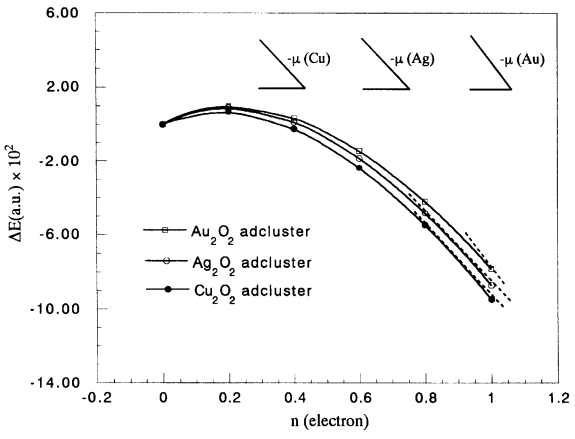

Fig. 6. $E(n)$ curves for the Cu_2O_2, Ag_2O_2, and Au_2O_2 adclusters in the highest spin coupling model at the optimized end-on geometries as shown in Table 1.

oxygen is explained by the DAM as being due to its poor donating property.

We note that the behavior of the $E(n)$ curve for the Au_2O_2 adcluster is just one of the cases already shown in Refs. [56,57]. That is, it is difficult for electron flow to occur between the clean bulk metal and the adcluster because it does not satisfy the condition clarified by the DAM [39]. However, as the energy at $n=1.0$ is lower than that at $n=0.0$, the electron transfer can be realized if the chemical potentials μ of the gold metal can be lowered by the addition of promoters, etc. Experimentally, the recent work performed by Haruta and coworkers [7,8] shows that gold is remarkably active for the oxidation of CO and hydrocarbons when it is supported on suitable metal oxides. This may be explained by the effect of the metal-oxide support.

The chemical potential of Au is much larger than those of Cu and Ag. We note that this difference is attributed actually to the relativistic effect in gold [58,59]. The importance of relativistic effects to the valence-electron properties such as chemical shift has recently been clarified in this laboratory [60–66].

5. Dissociative adsorption of O_2

Many experimental studies have shown that the dissociative adsorption of O_2 occurs on Cu and Ag surfaces, but not on an Au surface. This difference may explain the catalytic activities of these metals for the formation of formaldehyde from methanol [3–6]. We previously studied theoretically the dissociation of molecularly adsorbed oxygen on an Ag surface [34]. In this section, we examine the dissociation of O_2 on Cu and Au surfaces. We use an M_4O_2 adcluster with M_4 being a linear chain cluster instead of the M_2O_2 adcluster used in Section 4, because the surface size represented by M_2 is too small to describe the dissociation of O_2 on it, as described previously in some detail [34].

Fig. 7 shows the PECs for the low-lying states of the Cu_4O_2 adcluster ($n=1$) for an elongation of the O–O distance. The Cu–Cu distance was fixed at 2.556 Å, and the Cu–O distance was fixed

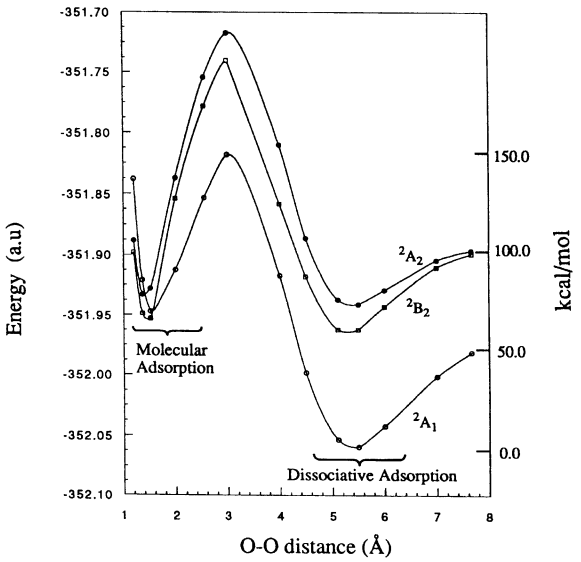

Fig. 7. PECs calculated by the SAC/SAC-CI method for the lowest three states in the O–O dissociation process of the Cu_4O_2 adcluster with $n=1$.

at the optimized side-on geometry of M_2O_2. The O–O distance was elongated from 1.20 to 7.66 Å, keeping the C_{2v} symmetry. There are three states, $^2A_1$, $^2A_2$, and $^2B_2$, in the lower energy region, and there are two potential minima for the three states; one is around the O–O distance of 1.35–1.55 Å, corresponding to the molecular adsorption states, and the other is around 5.11–5.50 Å, corresponding to the dissociative adsorption states. Among the molecular adsorption states, the $^2A_1$ state corresponds to the peroxide species, and the $^2A_2$ and $^2B_2$ states correspond to the superoxide species, the open orbitals being in-plane π^* for $^2B_2$ and out-of-plane π^* for $^2A_2$. The most stable dissociative adsorption state is $^2A_1$. It is 66 kcal mol^{-1} more stable than the molecular adsorption state. Although the $^2A_2$ and $^2B_2$ states also have the potential minima corresponding to the dissociative adsorption state, the energies are higher than that of the $^2A_1$ species by 72.5 kcal mol^{-1} and 56.7 kcal mol^{-1} respectively. These features of the PECs are similar to those obtained for the Ag_4O_2 system [34].

Similar calculations were also performed for the Au_4O_2 system: the results are listed in Table 5 together with those for the Cu_4O_2 and Ag_4O_2

Table 5
Energetics, net charges, and bond lengths of the dissociated oxygen on Cu, Ag, and Au surfaces calculated by M_4O_2 DAM and the SAC/SAC-CI method

System	Barrier[a] (kcal mol^{-1})	ΔE[b] (kcal mol^{-1})	Net charge (per O)	R_{O-O} (Å)	R_{M-O} (Å)
Cu_4O_2	84.9	66.6	−1.00	5.11	1.94
	Exptl.[c]				1.81–2.05
Ag_4O_2 [d]	77.0	44.0	−0.98	5.78	2.16
	Exptl.	40.8–44.0[e]			2.01–2.17[f]
Au_4O_2	94.8	−5.6	−0.68	5.77	2.18

[a] Energy barrier from molecular to dissociative adsorption.
[b] Stabilization energy from molecular to dissociative adsorption: $\Delta E = E$(dissociative adsorption) − E(molecular adsorption).
[c] Ref. [1].
[d] Ref. [34].
[e] Ref. [14].
[f] Ref. [13].

systems. The energy barriers between the molecular and dissociative adsorption states were calculated to be 84.9 kcal mol^{-1}, 77.0 kcal mol^{-1}, and 94.8 kcal mol^{-1} for the Cu_4O_2, Ag_4O_2, and Au_4O_2 systems respectively. The calculated energy barriers are much larger than the experimental result [14]. A reason may be due to the smallness of the cluster used here, but another possible reason is due to the surface dependence of the barrier. It was shown experimentally that the Cu(110) and Ag(110) surfaces can easily lead to the dissociative adsorption of O_2, but the Cu(111) and Ag(111) surfaces cannot [1]. The present high barriers may correspond to the results for the (111) surfaces, since in the present M_4O_2 adcluster one cannot simulate the effect of the ditch existing on the (110) surface. The activation energy barriers are calculated to be much smaller than the present ones when the larger M_{10}(110) and M_{12}(110) clusters are adopted [67]. The stabilization energies for the change from molecular to dissociative adsorptions are calculated to be 66.6 kcal mol^{-1}, 44.0 kcal mol^{-1}, and −5.6 kcal mol^{-1} for the Cu_4O_2, Ag_4O_2, and Au_4O_2 systems respectively. This result implies that the dissociative adsorption of O_2 occurs most easily on Cu, and next on Ag, but not on Au. This result agrees with the trend observed experimentally.

The net charges on the dissociated oxygen atom are 1.00, 0.98, and 0.68 on the Cu, Ag, and Au surfaces respectively: the values on the Cu and Ag surfaces are very close to each other and larger than that on the Au surface. This is due to the lower electron donating ability of the Au surface, as mentioned above.

The minimum of the dissociative adsorption state in Fig. 7 corresponds to the atomic oxygen adsorbed on the bridge site of the copper surface. To examine the reliability of this structure, we further optimized the Cu–O distance at this geometry by the SAC/SAC-CI method. The calculated Cu–O distance was 1.94 Å, which lies within the observed range of 1.81–2.05 Å [1]. The Cu–O distance of 1.94 Å is smaller than the Ag–O distance of 2.16 Å, obtained in the previous study [34], as expected from the difference in the bonding radii. This difference results in a stronger interaction between Cu and O, as seen already in the interaction between the copper surface and molecular peroxide. The differences in the electron donating abilities and in the bonding radii of the Cu, Ag, and Au metals explain the differences in the stabilities between the molecular and dissociative adsorption species, as well as those between the superoxide and peroxide species.

6. Conclusions

We have studied the stabilities and activities of the oxygen species adsorbed on Cu, Ag, and Au surfaces by the DAM combined with the

SAC/SAC-CI method. For molecular adsorption, both end-on and side-on geometries were investigated. The ground-state electronic structure of the molecularly adsorbed O_2 species in the end-on form is the superoxide O_2^-, and that in the side-on form is the peroxide O_2^{2-}. The end-on superoxide species is attributed in the previous study to be an active species for the partial oxidation of ethylene on an Ag surface.

The reactivities of the superoxide species on Cu, Ag, and Au surfaces for ethylene are very similar, giving smoothly ethylene oxide. The barriers leading to complete oxidation are equally high. The differences among Cu, Ag, and Au surfaces are small, if the superoxide species exists on the metal surfaces. The large differences observed in the catalytic activities of these metal surfaces are therefore attributed to the different stabilities of the adsorbed oxygen species, particularly the stability of the superoxide species.

The electron transfer from metal to O_2 is a key factor for the chemisorption of oxygen on a metal surface, as shown previously [34–37]. The differences in the relative stabilities of different oxygen species on different metal surfaces are attributed to the differences in the electron-donating abilities. The present DAM calculations show that, for Cu and Ag surfaces, one-electron transfer from the bulk metal into the adcluster occurs after some barriers. On the other hand, it is difficult for electron transfer to occur for Au surface, since the gold surface has a higher work function. This is why molecular adsorption of O_2 does not occur on the Au surface.

On Cu surface, peroxide is much more stable than superoxide and there is essentially no barrier for the conversion from superoxide to peroxide, so that the lifetime of the superoxide species should be too short to react with ethylene. On Ag surface, however, the superoxide species would have a considerable lifetime on the surface. On Au surface, the superoxide species does not exist, because the molecular adsorption of O_2 does not occur owing to the difficulty of the electron transfer from the clean bulk metal. We think that this difference in the stability of the end-on superoxide species on Cu, Ag, and Au surfaces is the reason for the difference observed in the catalytic activity of these metals for the partial oxidation of ethylene.

The mechanism of the dissociation of O_2 on a Cu surface is similar to that on an Ag surface studied previously [34]. The stable geometry is at a bridge site in the copper surface, and the calculated Cu–O distance of 1.94 Å agrees well with the experimental value of 1.81–2.05 Å. The dissociative state on the Cu surface is calculated to be more stable than that on the Ag surface. On the other hand, on the Au surface the dissociative adsorption does not occur, since its precursor state, i.e. molecular adsorption, does not occur, as shown in this paper.

Finally, the most important result of the present study is as follows. The above conclusion for the origin of the different catalytic activity of Cu, Ag, and Au surfaces for the partial oxidation of ethylene suggests a possibility of making a new catalyst for this reaction. The key is an appropriate lifetime of the end-on superoxide species on the metal. Silver realizes it without any special modification. However, if one can realize such superoxide species on some metals using some modification, we think that the essential factor is realized. For example, gold may become a catalyst by modifying it to give a larger electron donating ability to O_2.

Acknowledgements

We thank the referee for valuable comments. Some calculations were performed using the computers at the Institute for Molecular Science. Part of this study was supported by a Grant-in-Aid for Scientific Research from the Japanese Ministry of Education, Science, and Culture and by the New Energy and Industrial Technology Development Organization (NEDO).

References

[1] F. Besenbacher, J.K. Nørskov, Prog. Surf. Sci. 44 (1993) 5. M.A. Lazaga, D.T. Wickham, D.H. Parker, G.N. Kastanas, B.E. Koel, Am. Chem. Soc. Symp. Ser. (1993) 90.
[2] M. Haruta (organizer), Workshop on Environmental Catalysis: The Role of IB Metals Proceedings, November 2–3, 1995, Ikeda, Oaka, Japan.
[3] M.D. Thomas, J. Am. Chem. Soc. 42 (1920) 867.

[4] K. Wu, D. Wang, X. Wei, Y. Cao, X. Guo, Surf. Sci. 304 (1994) L481.
[5] I.E. Wachs, R.J. Madix, Surf. Sci. 76 (1978) 531.
[6] X. Bao, J. Deng, J. Catal. 99 (1986) 391.
[7] M. Haruta, S. Tsubota, T. Kobayashi, M. Kageyama, M. Genet, B. Delmon, J. Catal. 144 (1993) 175.
[8] T. Hayashi, M. Haruta, Shokubai 37 (1995) 72 (in Japanese). M. Haruta, Chem. Eng. 59 (1995) 168 (in Japanese).
[9] H. Nakatsuji, H. Nakai, K. Ikeda, Y. Yamamoto, Surf. Sci., in press.
[10] A. Sexton, R.J. Madix, Chem. Phys. Lett. 76 (1980) 294. M.A. Bartreau, J. Madix, Chem. Phys. Lett. 97 (1983) 85.
[11] C. Backx, C.P.M. de Groot, P. Biloen, Surf. Sci. 104 (1981) 300.
[12] C. Pettenkofer, I. Pockrand, A. Otto, Surf. Sci. 135 (1983) 52. C. Pettenkofer, J. Eickmans, U. Erturk, A. Otto, Surf. Sci. 151 (1985) 9.
[13] A. Pushmann, J. Haase, Surf. Sci. 144 (1984) 559.
[14] C.T. Campbell, M. Paffett, Surf. Sci. 143 (1984) 517. C.T. Campbell, Surf. Sci. 157 (1985) 43.
[15] K. Bange, T.E. Madey, J.K. Sass, Chem. Phys. Lett. 113 (1985) 56.
[16] K.C. Prince, G. Paolucci, A.M. Bradshaw, Surf. Sci. 175 (1986) 101.
[17] J. Stohr, D.A. Outka, Phys. Rev. B 35 (1987) 4119.
[18] P.J. van der Hoek, E.J. Baerends, Surf. Sci. 221 (1989) L791.
[19] A. Spitzer, H. Luth, Surf. Sci. 118 (1982) 121; 136.
[20] K. Prabhakaran, P. Sen, C.N.R. Rao, Surf. Sci. 177 (1986) L971. M.K. Rajumon, K. Prabhakaran, C.N.R. Rao, Surf. Sci. Lett. 233 (1990) L237.
[21] J.M. Mundenar, A.P. Baddorf, E.W. Plummer, L.G. Sneddom, R.A. Didio, D.M. Zehner, Surf. Sci. 188 (1987) 15.
[22] A. Hodgson, A.K. Lewin, A. Nesbitt, Surf. Sci. 293 (1994) 211.
[23] M.A. Chesters, G.A. Somorjai, Surf. Sci. 52 (1975) 21.
[24] D.D. Eley, P.B. Moore, Surf. Sci. 76 (1978) L599.
[25] J.J. Pireaux, M. Chtaib, J.P. Delrue, P.A. Thiry, M. Liehr, R. Caudano, Surf. Sci. 141 (1984) 211.
[26] A.G. Sault, R.J. Madix, Surf. Sci. 169 (1986) 347.
[27] J.H. Lin, B.J. Garrison, J. Chem. Phys. 80 (1984) 2904.
[28] A. Selmani, J.M. Sichel, D.R. Salahub, Surf. Sci. 157 (1985) 208.
[29] M.L. Mckee, J. Chem. Phys. 87 (1987) 3143.
[30] T.H. Upton, P. Stevens, R.J. Madix, J. Chem. Phys. 88 (1988) 3988.
[31] E.A. Carter, W.A. Goddard III, Surf. Sci. 209 (1989) 243; J. Catal. 112 (1988) 80.
[32] K. Broomfiled, R.M. Lambert, Mol. Phys. 66 (1989) 421.
[33] P.J. van den Hoek, E.J. Baerends, R.A. van Santen, J. Phys. Chem. 93 (1989) 646.
[34] H. Nakatsuji, H. Nakai, Chem. Phys. Lett. 174 (1990) 283; J. Chem. Phys. 98 (1993) 2423.
[35] H. Nakatsuji, H. Nakai, Can. J. Chem. 70 (1992) 404.
[36] A. Wander, Surf. Sci. 216 (1989) L347.
[37] B. Hellsing, S. Gao, Chem. Phys. Lett. 187 (1991) 137.
[38] J.M. Ricart, J. Torras, A. Clotet, J.E. Sueiras, Surf. Sci. 301 (1994) 89.
[39] H. Nakatsuji, J. Chem. Phys. 87 (1987) 4995.
[40] H. Nakatsuji, H. Nakai, Y. Fukunishi, J. Chem. Phys. 95 (1991) 640.
[41] H. Nakatsuji, K. Hirao, J. Chem. Phys. 68 (1978) 2053.
[42] H. Nakatsuji, Chem. Phys. Lett. 59 (1978) 362; Chem. Phys. Lett. 67 (1979) 329.
[43] H. Nakatsuji, Acta Chim. Hung. 129 (1992) 719.
[44] H. Nakatsuji, in: J. Leszczynski (Ed.), Computational Chemistry – Reviews of Current Trends, vol. 2, World Scientific, London, 1997.
[45] Handbook of Chemistry and Physics, CRC Press, Cleveland, OH, 1984–1985.
[46] H. Nakatsuji, Chem. Phys. 75 (1983) 425.
[47] M. Dupuis, A. Farazdel, Program System HONDO8 from MOTECC-91, 1991.
[48] H. Nakatsuji, Program system for SAC and SAC-CI calculations, Program Library No. 146 (Y4/SAC), Data Processing Center of Kyoto University, 1985; Program Library SAC85, No. 1396, Computer Center of the Institute for Molecular Science, 1981.
[49] P.J. Hay, W.R. Wadt, J. Chem. Phys. 82 (1985) 270.
[50] S. Huzinaga, J. Chem. Phys. 42 (1965) 1293.
[51] T.H. Dunning Jr., J. Chem. Phys. 53 (1970) 2823.
[52] T.H. Dunning Jr., P.J. Hay, in: H.F. Schaeffer III (Ed.), Modern Theoretical Chemistry, vol. 3, Plenum, New York, 1977.
[53] S. Huzinaga, J. Andzelm, M. Klobukowski, E. Radzio-Andzelm, Y. Sakai, H. Tatewaki, Gaussian Basis Sets for Molecular Calculations, Elsevier, New York, 1984.
[54] P.J. Hay, R.L. Martin, J. Chem. Phys. 83 (1985) 5174.
[55] P.H. Krupenie, J. Phys. Chem. Ref. Data 1 (1972) 423.
[56] H. Nakatsuji, R. Kuwano, H. Morita, H. Nakai, J. Mol. Catal. 82 (1993) 211.
[57] H. Nakatsuji, Prog. Surf. Sci. 54 (1997) 1.
[58] E. Eliav, U. Kaldor, Y. Ishikawa, Phys. Rev. A 49 (1994) 1724.
[59] U. Kaldor, B.A. Hess, Chem. Phys. Lett. 230 (1994) 1.
[60] H. Nakatsuji, H. Takashima, M. Hada, Chem. Phys. Lett. 233 (1995) 95.
[61] H. Nakatsuji, H. Takashima, M. Hada, Chem. Phys. Lett. 233 (1995) 13.
[62] H. Nakatsuji, T. Nakajima, M. Hada, H. Takashima, S. Tanaka, Chem. Phys. Lett. 247 (1995) 418.
[63] H. Nakatsuji, M. Hada, T. Tejima, T. Nakajima, Chem. Phys. Lett. 249 (1996) 284.
[64] H. Kaneko, M. Hada, S. Tanaka, H. Nakatsuji, Chem. Phys. Lett. 261 (1996) 1.
[65] C.C. Ballard, M. Hada, H. Kaneko, H. Nakatsuji, Chem. Phys. Lett. 254 (1996) 170.
[66] H. Nakatsuji, M. Hada, H. Kaneko, C.C. Ballard, Chem. Phys. Lett. 255 (1996) 195.
[67] Z.M. Hu, H. Nakai, K. Ikeda, H. Nakatsuji, in preparation.